JOURNAL OF SOLID STATE CHEMISTRY 104, 289–301 (1993)

A Novel Bismuth Cuprate, $Bi_{14+x}Sr_7Ba_7Cu_{7-x}O_{42+x/2}$, Seventh Member of a Structural Series, $(Bi_2A_2CuO_6)_{n-2}$ $(Bi_{4+x}A_4Cu_{2-x}O_{12+x/2})$, Related to the 2201 Bismuth Cuprates

M. HERVIEU, C. MICHEL, A. Q. PHAM, AND B. RAVEAU

Laboratoire CRISMAT, CNRS URA 1318, ISMRa Université de Caen, Boulevard du Maréchal Juin, 14050 Caen Cedex, France

Received July 6, 1992; in revised form October 13, 1992; accepted October 14, 1992

A new bismuth based cuprate has been synthesized with composition $Bi_{15}Sr_7Ba_7Cu_6O_{42.5}$. It crystallizes in a monoclinic cell with a = 20.121 (5) Å, b = 5.509 (1) Å, c = 25.736 (10) Å, β = 111°08 (2), and the possible space groups are A_2, A_m and $A_{2/m}$. A high resolution electron microscopy study showed that its structure results in a periodic rupture of infinite layers similar to those observed in the "2201" modulated superconducting oxide; it involves a sharing mechanism along **c** forming 2201-type ribbons seven polyhedra wide. A new family of oxides, the "collapsed" 2201-type bismuth cuprates, is described, $(Bi_2A_2CuO_6)_{n-2}$ $(Bi_{4+x}A_4Cu_{2-x}O_{12+x/2})$, this oxide being the n = 7 member. The existence of defective member n' = 6 has been shown, which sometimes results in regular local intergrowth [6/7]. The close structural relationships with the 2201 modulated phase is illustrated by the easy junction between the two structures. No superconducting behavior has been detected.

Introduction

After the discovery of superconductivity in the system Bi–Sr–Cu–O (*1*), an extensive work was devoted all over the world to the bismuth based cuprates. The ideal structure of the corresponding phase (Fig. 1a), $Bi_2Sr_2CuO_{6+\delta}$, has never been observed so far: it was indeed shown that the XRD and ED patterns (*2–8*) of this oxide exhibit incommensurate satellites. The recent resolution of the structure of this cuprate from a single crystal (*9*) has confirmed that it derives from the idealized structure by a modulated distribution of the different cations, coupled with incommensurate displacements. Thus the actual monoclinic modulated structure of $Bi_2Sr_2CuO_{6+\delta}$ (Fig. 1b) consists of undulated bismuth and strontium distorted rock salt layers stacked with single octahedral copper layers.

In fact the Bi–Sr–Cu–O system is characterized by a very complicated crystal chemistry in which the ideal structure "$Bi_2Sr_2CuO_6$" is the starting point for the generation of numerous closely related oxides as well from the chemical as from the structural view point. Besides this cuprate, a second oxide, called the 2201-collapsed monoclinic phase, was synthesized (*10*, *11*), to which the composition $Bi_{17}Sr_{16}Cu_7O_{49-x}$ was attributed. The structural model of this phase (*10*) is deduced from the 2201-ideal structure (Fig. 1a) by a periodic rupture of the infinite layers; i.e., by a sharing mechanism along **c**, forming 2201-type ribbons eight copper octahedra wide, shifted with respect to each other along **c** (Fig. 2). The third structural type applies to the orthorhombic tubular copper oxides, with general formulation $(Bi_{2+x}Sr_{2-x}CuO_6)_n$ (*12–15*), which form a large family with n ranging from 4 to 7 (*14*). The structure of these phases (Fig. 3) can be described from the intergrowth of ideal 2201-type ribbons which are n copper octahedra wide with sin-

0022-4596/93 $5.00

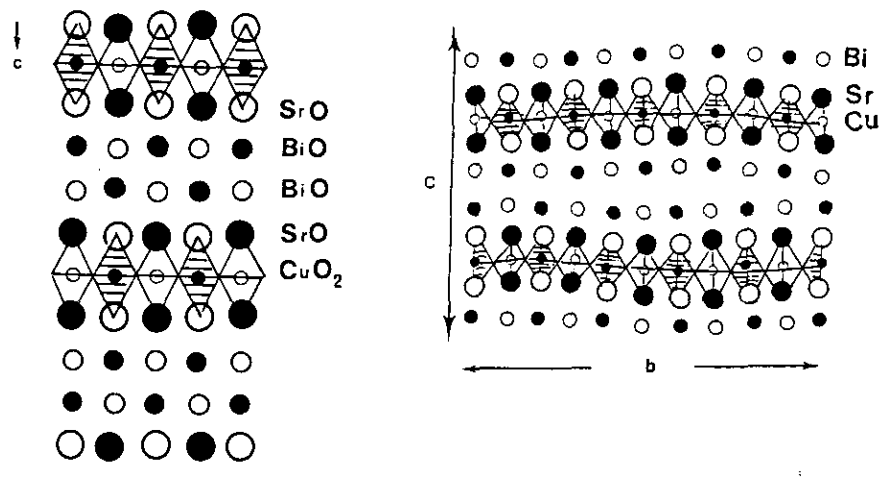

FIG. 1. Idealized drawing of (a) the ideal 2201-type structure and (b) the modulated 2201 structure.

gle oxygen deficient copper layers which are orthogonal to the 2201 initial layers; as a result large channels are formed where "Bi–O" ribbons are located. A fourth structure, with approximate composition $Bi_{13}Sr_{19.5}Cu_{13}O_{52}$ was recently characterized (*16*), called monoclinic 2201 tubular phase, whose structure (Fig. 4) corresponds to a translation of one bismuth layer with respect to the next one. Regular intergrowths of such monoclinic tubular ribbons with tubular orthorhombic ribbons were locally observed by HREM. The very close relationships between these structures cause numerous extended defects to be observed by HREM (*15*).

The complete substitution of barium for strontium in the 2201-type oxide $Bi_2Ba_{2-x}La_xCuO_{6+\delta}$ was recently achieved (*17*) with a modulated structure whereas the lead substituted oxides $Bi_{2-x}Pb_xBaLaCuO_{6-\delta}$ (*18*) showed the coexistence of two 2201-type

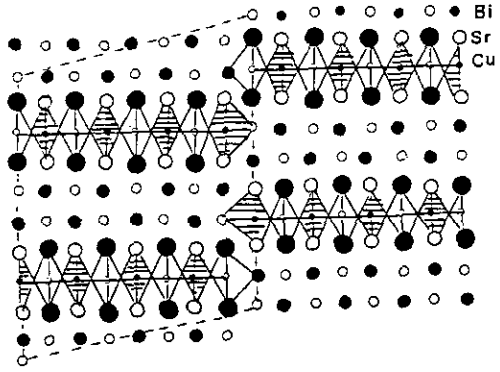

FIG. 2. Idealized drawing of the 2201-"collapsed" phase.

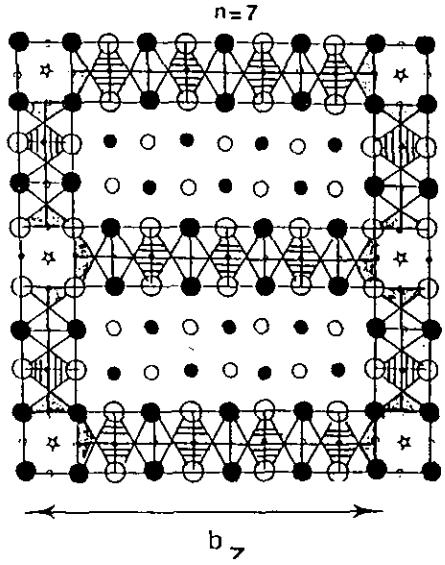

FIG. 3. Idealized drawing of the $n = 7$ member of the orthorhombic tubular phase.

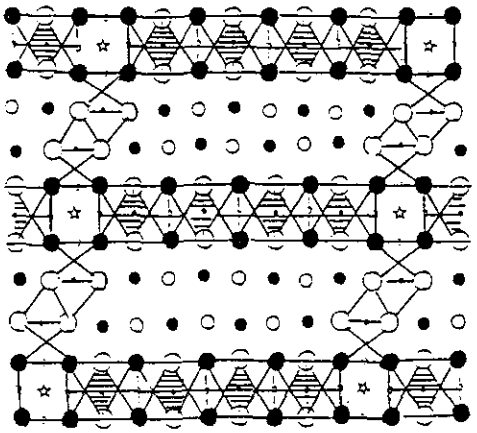

FIG. 4. Idealized drawing of the member $n = 7$ of the monoclinic tubular phase.

phases, modulated and nonmodulated, respectively. This paper deals with the synthesis and structural characterization of an original phase, $Bi_{14+x}Sr_7Ba_7Cu_{7-x}O_{42+x/2}$ ($x \sim 1$), seventh member of a new series of cuprates $(Bi_2A_2CuO_6)_{n-2}(Bi_{4+x}A_4Cu_{2-x}O_{12+x/2})$, related to the monoclinic 2201-collapsed phase, with A = Ba, Sr.

Experimental

Samples were prepared according to the general formulation $Bi_{2n+x}Ba_{2n-y}Sr_yCu_{n-x}$ with $n = 7$, y varying between 0 and 14 and x between 0 and 2. The starting materials were Bi_2O_3, CuO, $SrCO_3$, and $Ba(OH)_2$, $8H_2O$. The mixtures were intimately ground, pressed in the form of pellets, and heated at 750°C for 24 hr in a nitrogen flow. After this thermal treatment, the pellets were ground, repelletized, and heated again for 24 hr under the same conditions. The X-ray powder diffraction patterns were registered with a Seifert vertical goniometer equipped with a primary monochromator to select the $CuK\alpha_1$ radiation. Data were collected in the range $10 \leq 2\theta \leq 90°$ by step scanning with increment of 0.02° (2θ). Lattice constants were determined by a classical least squares refinement program.

The electron microscopy study was carried out using a JEOL 200 CX electron microscope, operating at 200 kV and fitted with a side entry goniometer (±60°). The high resolution electron microscopy study was performed using a TOPCON 2B electron microscope.

Results

The powder X-ray diffraction patterns show that a single phase is obtained for $x \sim 1$ and for $y \sim 5$–7. Nevertheless the limits cannot be determined with accuracy owing to the formation of traces of $BaCO_3$ and of 2201-type phase. Owing to the great complexity of the X-ray patterns (Fig. 5), an electron diffraction investigation was systematically carried out. The grains are well crystallized and exhibit a mica-like morphology; this is a classical feature of the bismuth-rich oxides with a 2201-related structure.

The reconstruction of the reciprocal space, performed on numerous crystals, gives evidence of a monoclinic cell with the parameters

$$a = \tfrac{7}{2} x a_{2201}/\cos(\beta\text{-}90°)$$

$$b \sim a_p\sqrt{2} \sim a_{2201}$$

$$c \sim 26 \text{ Å} \sim c_{2201}$$

$$\beta \sim 111°,$$

where a_p is the parameter of the ideal cubic perovskite cell and a_{2201} and c_{2201} are the parameters of the ideal tetragonal cell of 2201 structure (Fig. 1a). The conditions of existence of the reflections are $hkl: k + l = 2n$ involving the possible space groups $A_{2/m}$, A_m, and A_2.

The cell parameters were then refined from the X-ray powder diffraction patterns, with

$$a = 20.121\ (5)\ \text{Å};\ b = 5.509\ (1)\ \text{Å};$$
$$c = 25.736\ (10)\ \text{Å};\ \beta = 111°08(2).$$

The [001] and [010] electron diffraction patterns are shown in Figs. 6a and b. On the [001] pattern (Fig. 6a), the strong reflections

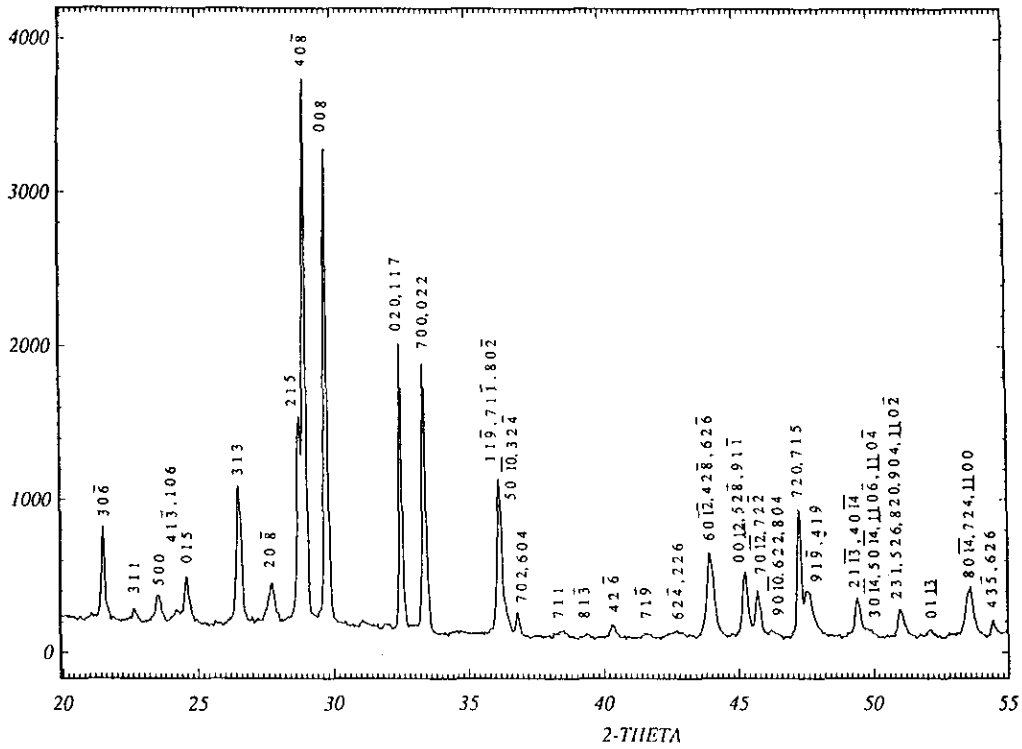

FIG. 5. Powder X ray diffraction pattern (Cu$K\alpha_1$ radiation) for the nominal composition $Bi_{15}Sr_{6.5}Ba_{7.5}Cu_6O_{42.5}$, with Miller indices.

are characteristic of the F-type 2201 cell. Along the **A** axis, extra spots are observed, leading to a "$7 \times a_p\sqrt{2}/2$" superstructure. From comparison with the other [001] E.D. patterns of the different phases of the Bi–Sr–Cu–O system, such a pattern can be considered as representative of a "collapsed" 2201-type structure. However, the periodicity along **a** is different from that described by Takano and co-workers (*10*) for the pure strontium collapsed phase ($a \sim 4\ a_p\sqrt{2}$). In the 2201-collapsed monoclinic phase, $Bi_{17}Sr_{16}Cu_7O_{49-x}$, the "$4 \times a_p\sqrt{2}$" superstructure is the result of the presence of eight-octahedra-wide 2201 ribbons shifted with respect to each other along **c** (Fig. 2); consequently in our Ba/Sr phase similar ribbons shifted along **c** can be proposed but with a periodicity of seven octahedra instead of eight (Fig. 7). The [010] lattice image (Fig. 8) is in agreement with this hypothesis, since it gives evidence of staggered slices, about 19 Å wide, translated along **c** of about 5 Å with respect to each other. Note also the existence of stacking defects corresponding to variations of the width of 2201-type ribbons (arrows in Fig. 8). Such defects result in small variations of the periodicity along **A** and the existence of weak streaks along **A** in the E.D. patterns (Fig. 6). The latter defects are discussed later.

HREM Study: A Structural Model for the Oxide $Bi_{14+x}Sr_7Ba_7Cu_{7-x}O_{12+x/2}$

Two [010] HREM images are given in Fig. 9. The contrast resulting from the nature of the layer stacking along **c** can be compared with those obtained for the superconductive 2201 oxides (*19*) since it shows clearly the existence of the following sequence: [(Ba, Sr)O]–[BiO]–[BiO]–[(Ba, Sr)O]-[CuO_2]. It

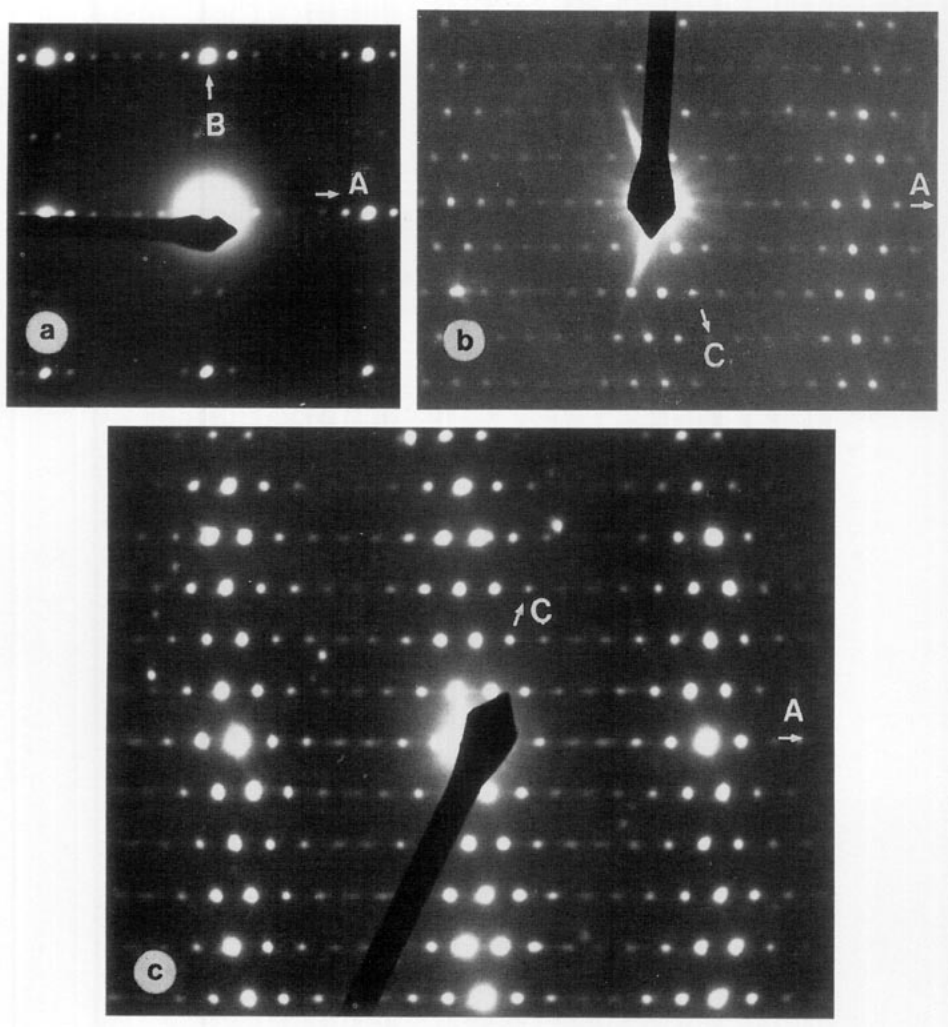

FIG. 6. (a) [001] and (b) [010] E.D. patterns of $Bi_{15}Ba_{7.5}Sr_{6.5}Cu_6O_{39.5}$. (c) when the number of defect is high, a small variation of the periodicity is observed along A, leading to reflections in incommensurate positions.

differs by the absence of modulation and the clear translation of a 2201 type slice, seven octahedra width, along the **c** axis. However, the existence of defects is observed for most of the crystals. The absence of data about atomic coordinates from XRD does not allow calculations of the theoretical images. However the close relationships with the 2201-modulated structure allow the simulated image of the latter to be used for our interpretation, taking also into consideration the model proposed by Takano and co-workers (*10*) for $Bi_{17}Sr_{16}Cu_7O_{39-x}$. Indeed the examination of the two enlarged HREM images with different focus values shows that the bismuth positions are correlated with the segments of seven darkest dots in Fig. 9a, and with those of seven bright spots in Fig. 9b. Consequently the "Ba, Sr" positions are correlated with segments of intermediate intensity in both images whereas copper positions are not visible on Fig. 9a, and are correlated with the darkest segments on Fig. 9b. From these

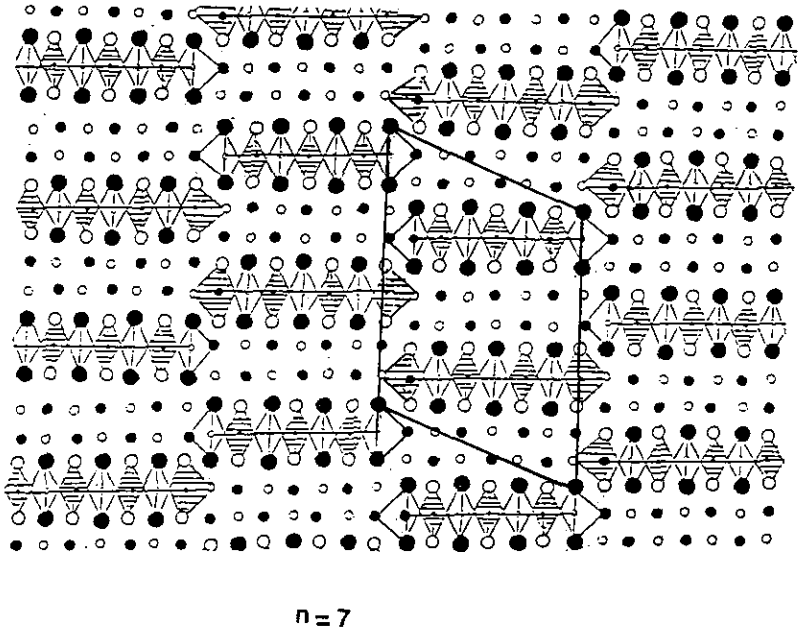

FIG. 7. Hypothetical structure of a member $n = 7$ of the "collapsed" phase.

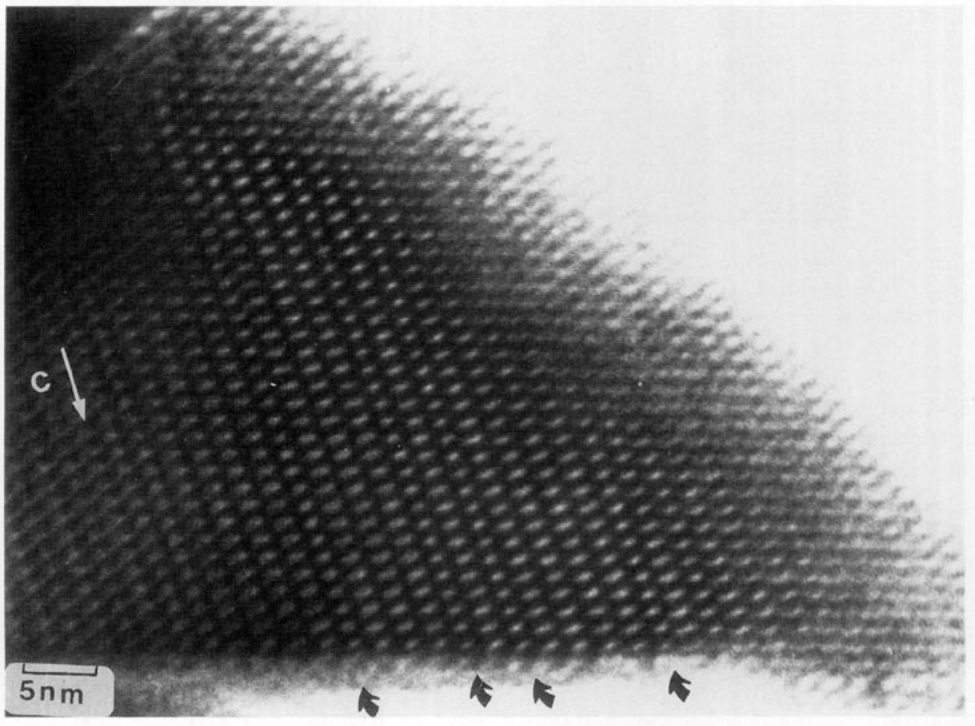

FIG. 8. [010] lattice image giving evidence of staggered slices.

enlarged HREM images the following comments can be made:

(i) The formation of 2201-type blocks, seven polyhedra wide, is evident in the thicker part of the crystals. But the important difference from the $Bi_{17}Sr_{16}Cu_7O_{49-x}$ oxide comes from the examination of the thin edge of the crystal which shows (Fig. 9b) that the cationic segments are not abruptly interrupted but form in fact strongly undulating layers in which cationic segments of different nature are connected.

(ii) One observes that a segment of "Bi" rows (dark and bright spots in Fig. 9a and 9b, respectively) is connected to a segment of "(Ba, Sr)" rows of one side (less dark spots in Fig. 9a) and to a segment of Cu rows (darkest spots in Fig. 9b) on the other side. In the same way a segment of "Ba Sr" rows is connected on one side to an other segment Ba(Sr) rows and on the other side to a segment of "Bi" rows.

(iii) At the junction between two segments forming the undulating layers parallel to (001) (Fig. 9), the cations are strongly displaced. The interruption between two 2201-type ribbons along **a** is not abrupt, but suggests parallel exchanges between cations at the junction; i.e., local substitutions between Bi, Ba(Sr), and Cu.

As a result, a schematic drawing deduced from these images and corresponding to the different Bi, Ba/Sr, and Cu ribbons can be proposed (Fig. 9c); it shows the existence of slices of 2201 type which are seven Bi (or Cu or Ba/Sr) polyhedra wide (instead of eight for $Bi_{17}Sr_{16}Cu_7O_{39+x}$) and is in agreement with the idealized model proposed in Fig. 7. The [001] images (Fig. 10) do not allow any additional information about the distribution of the cations to be obtained owing to the fact that ions of different nature are superposed along **c**. Nevertheless they show that two layers (double white lines) are involved at the junction between the two 2201-ribbons.

The EDS semiquantitative analysis, performed on about 50 crystals, leads to the composition "$Bi_{15.2}(Ba,Sr)_{13.9}Cu_{5.9}O_z$", with a Ba/Sr ratio slightly larger than 1. This analysis strongly supports the above model since it is indeed close to the theoretical formula deduced from the "$7 \times a_p\sqrt{2}/2$" superstructure, i.e., $(Bi_2SrBaCuO_{6+\delta})_7$; it only shows an excess bismuth with respect to copper, which is compatible with the HREM observations and can be explained by the junctions between the 2201-type ribbons.

It is in fact difficult to deduce the nature of the cations and of their environment from the HREM images. However, it seems that there does not exist a layer with a different structure at the boundary between two 2201-type ribbons, in contrast to the tubular phase; moreover, the contrast suggests that Bi, Sr, or Ba occupy preferentially the junction zone rather than copper, in agreement with the copper deficiency with respect to the formula $Bi_2A_2CuO_{6+\delta}$.

Thus, the structure of this cuprate appears as intermediate between the modulated 2201-type structure (Fig. 1b) and that of the nonmodulated phase $Bi_{17}Sr_{16}Cu_7O_{49-x}$ (Fig. 2). The presence of barium, much larger than strontium, may be at the origin of the undulation of the layers which is induced by the stereoactivity of the $6s^2$ lone pair of Bi(III), leading to an oval shape of two adjacent $(BiO)_7$ segments (Fig. 9c). From this structural study a general formulation $(Bi_2A_2CuO_6)_{n-2}(Bi_{4+x}A_4Cu_{2-x}O_{12+x/2})$ can be proposed for a new series of cuprates in which n corresponds to the number of polyhedra, which dictates the a parameter, and A is Ba or Sr (a small excess bismuth on the latter sites is also possible). The different members of this series should be built of 2201-type ribbons, which consists of ribbons of $(n-2)$ CuO_6 octahedra, connected at each junction by two distorted polyhedra in which the cationic distribution can be modified, i.e., Cu can be partly replaced by bismuth. In such structures, the connection between (BiO) and (SrO) layers will not involve any particular distortion owing to their ability to form rock salt layers, whereas the extension of one (BiO) by one

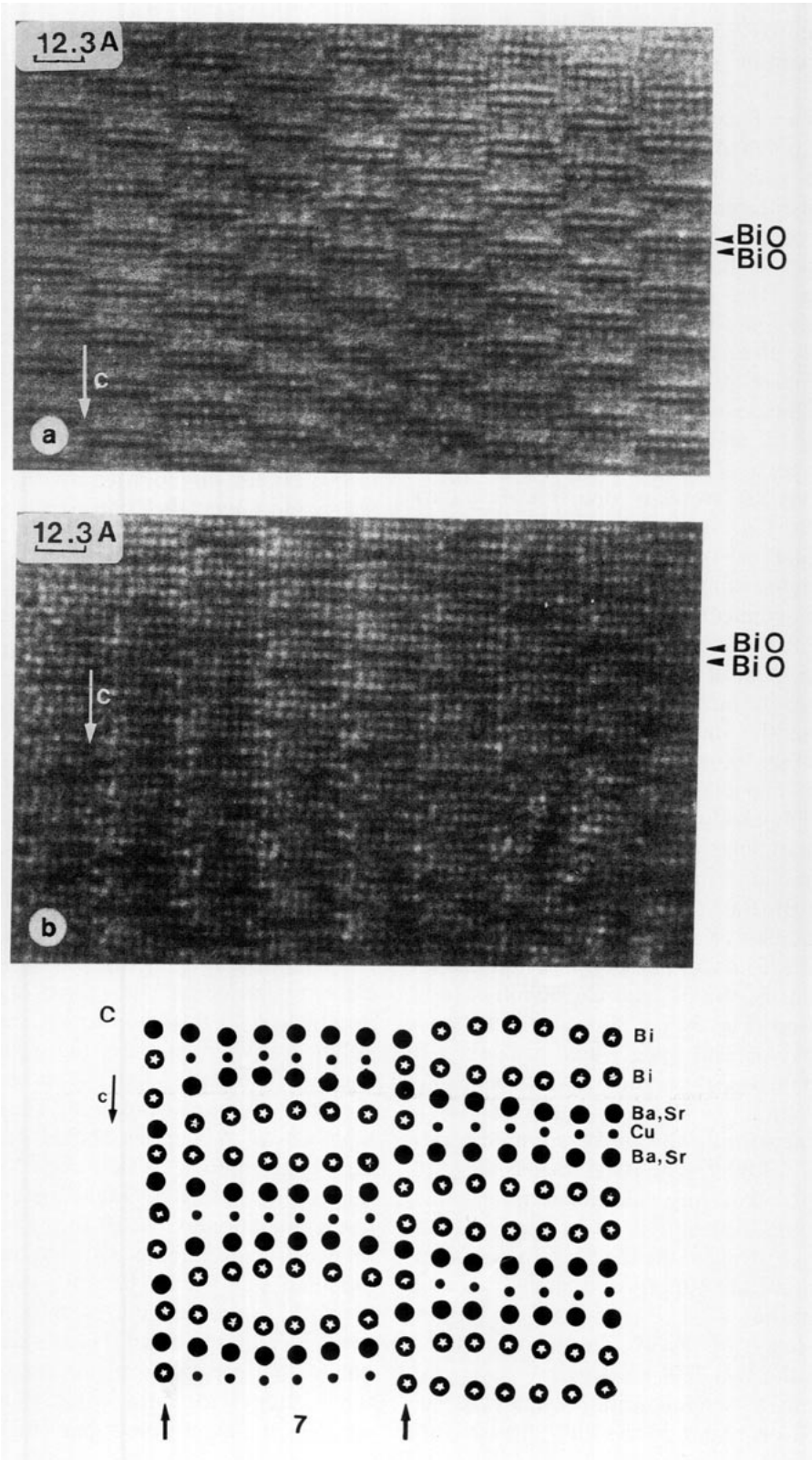
12.3 A
BiO
BiO
c
a
12.3 A
BiO
BiO
c
b
C
c
Bi
Bi
Ba,Sr
Cu
Ba,Sr
7

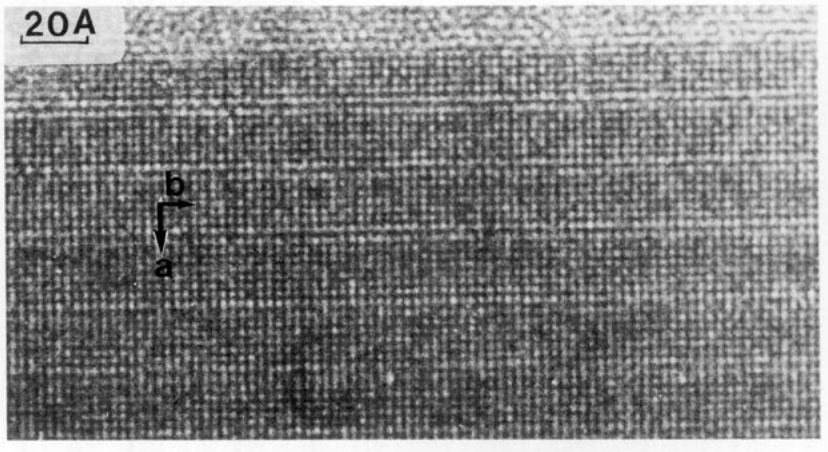

FIG. 10. Enlarged [001] image.

(CuO_2) layer is not obvious. The connection of the two adjacent layers through BiO_7 pentagonal bipyramids or CuO_5 trigonal bipyramids could be an explanation.

Thus, in this structural family, $Bi_{17}Sr_{16}Cu_7O_{49-x}$ represents the member $n = 8$, and $Bi_{15}(Ba, Sr)_{14}Cu_6O_{42.5}$ corresponds to the $n = 7$ member, both with $x \approx 1$; the values of the theoretical cell parameters of the different members of this series can be deduced from those of 2201-type structure according to the following relations:

$$a = na_p \frac{\sqrt{2}}{2} \times 1/\cos(\beta - 90°)$$

$$b = a_p \sqrt{2} = a_{2201}$$

$$c = c_{2201} = a_p(3\sqrt{2} + 2)$$

and

$$\tan(\beta\text{-}90°) = \frac{\sqrt{2} + 2}{2n} \text{ if } n \text{ is even}$$

$$\text{and} \quad \tan(\beta\text{-}90°) = \frac{\sqrt{2} + 1}{n} \text{ if } n \text{ is odd.}$$

Intergrowth Phenomena

The possibility of variation of the thickness of the 2201-type ribbons suggests the existence of intergrowth phenomena, characterized by the existence of defective members with n' different from the n value which characterizes the matrix. Indeed, as previously mentioned, rare are the crystals where such phenomena are not observed. The most frequent member observed as defect, corresponds to $n' = 6$ (see Fig. 8). In some crystals, regular intergrowths of $n = 7$ and $n' = 6$ members are observed along **a** (Fig. 11); in that image, the $[BiO]_\infty$ segments appear as dark rows and the undulations of the different layers, which form the structure, can be clearly seen as the interpenetration of the layers at the level of the junction. Such a regular member corresponds to a $n' = 6.5$ value whose a parameter is 20 times a_{2201} to preserve the periodicity.

Intergrowth defects involving large 2201-type ribbons are sometimes observed. An example is shown in Fig. 12 where $n'' = 19$ (arrowed); it can be noted that in this large slice the structure is modulated. Note also that these $n'' = 19$ modulated 2201-type slices are connected longitudinally to $n' = 6$ and $n = 7$ nonmodulated collapsed layers (left part of Fig. 12). In order to accomodate the n' defects to the n'' ones, the stacking of the nonmodulated collapsed layers must

FIG. 9. Enlarged [010] HREM image: (a) the [BiO] layers appears as row of white dots and the position of the cation is correlated to the white dots, (b) the positions of the bismuth atoms are correlated to the darkest dots, (c) schematic drawing deduced from these images.

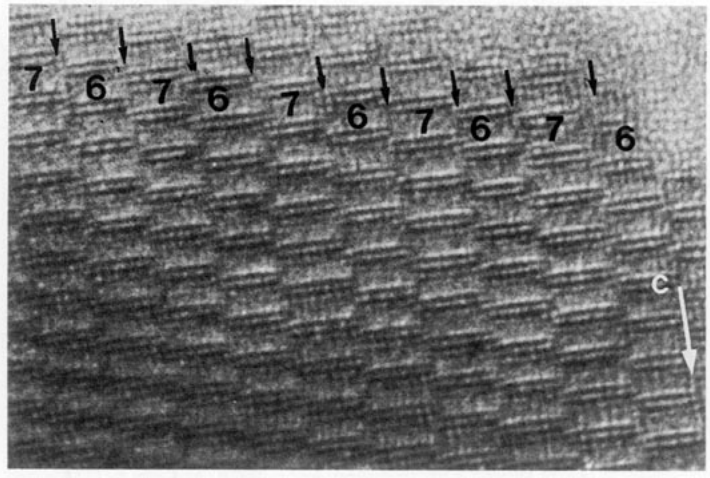

FIG. 11. Regular intergrowth of $n' = 6$ and $n = 7$ members.

obey the relation $n'' = \Sigma n'$; such a condition is obtained by the sequence $n' = 6, 6, 7$. In the same way, the modulated defective slice $n'' = 16$ (Fig. 13 left part) is prolonged (right part) by an assemblage of three nonmodulated collapsed layers $n'' = 5, 5, 6$. On this image, it can be seen that at the level of the connection, an additional layer is locally present to compensate for the shifting of the collapsed phase (curved arrow) (Fig. 13b).

Longitudinal intergrowth, corresponding to a variation of the thickness of the 2201-type modulated ribbons along **c** is some-

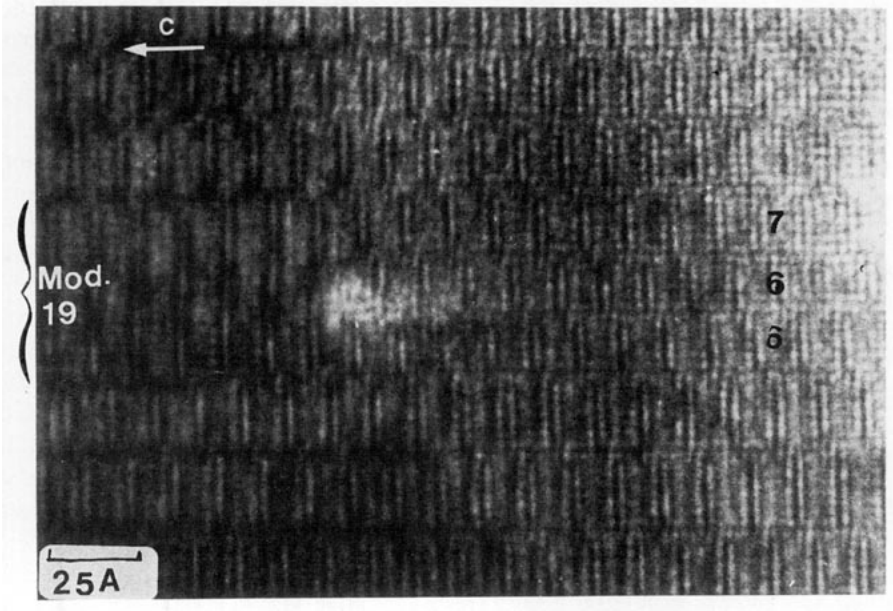

FIG. 12. [010] HREM image showing the coexistence of modulated phase (right part) with $n'' = 19$ and the collapsed phase.

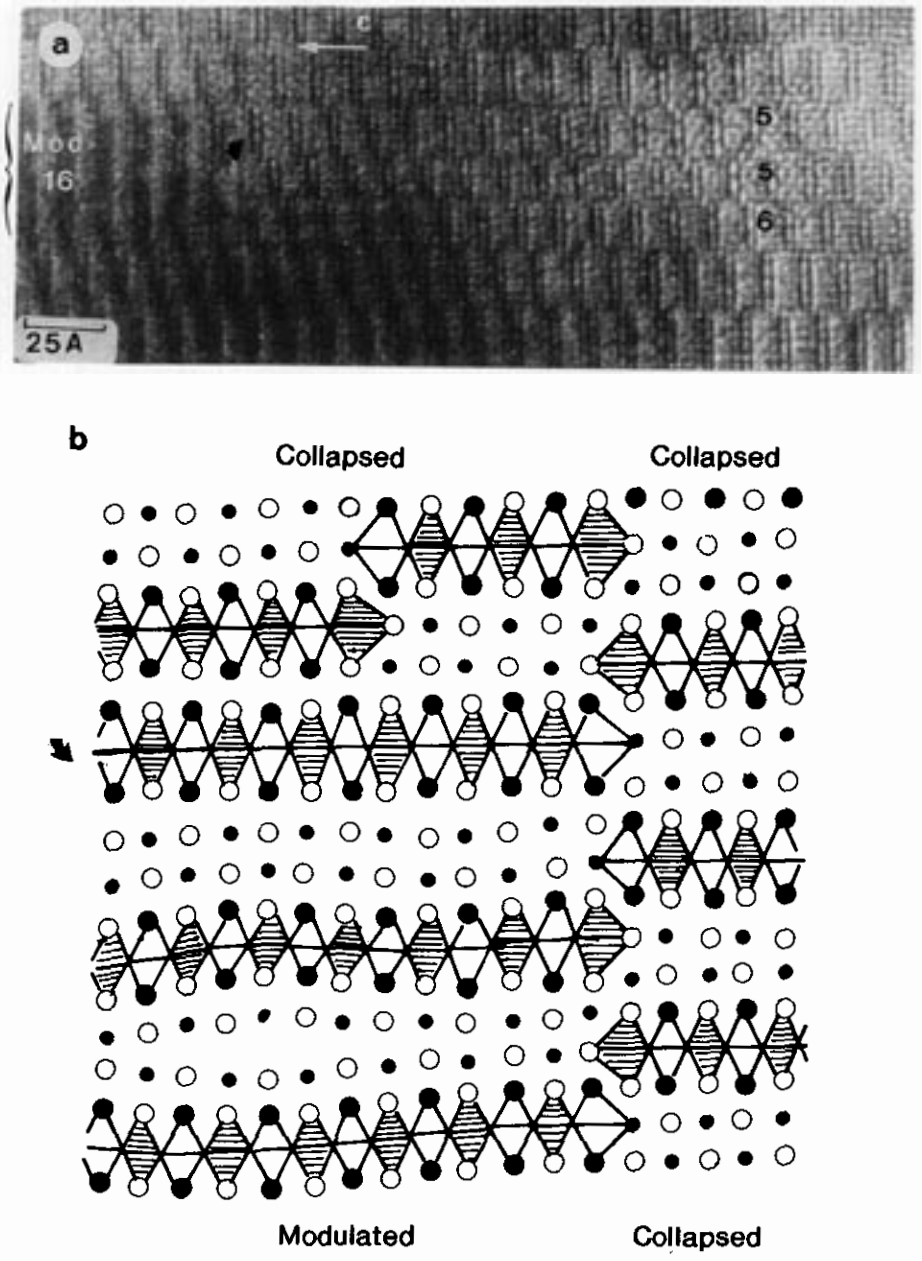

FIG. 13. (a) [010] HREM image where an $n'' = 16$ slice (right part) is prolonged by three $n' = 6$, 5, 5 members of the collapsed phase. (b) An additional layer is locally present to compensate for the shifting (curved arrow).

times observed. In this case, the junction boundaries seem to undulate; an example is shown in Fig. 14 (marked by white triangles). In such defects, regular members $n = 7$ are locally replaced by $n' = 6$ and $n' = 8$ members; this can be easily understood by a cation substitution at the level of the boundary.

Conclusion

The new phase, synthesized for a composition close to $Bi_{15}Ba_7Sr_7Cu_6O_{42.5}$, has been characterized by electron microscopy. The parameters were refined from the XRD data in an A-centered monoclinic cell with a = 20.121 (5) Å, b = 5.509 (1) Å, c = 25.736 (10) Å, and β = 111°08 (2). From the high resolution electron microscopy, the structure can be related to the "2201"-type in the layer stacking and to the "$Bi_{17}Sr_{16}Cu_7O_{49}$" type for the sharing mechanism along **c** which involves the formation of 2201-type ribbons. This original oxide can be described as a member n = 7 of a structural family $(Bi_2A_2Cu_7O_6)_{n-2}$ $(Bi_{4+x}A_4Cu_{2-x}O_{12+x/2})$. The existence of defective members with $n' \neq n$, the nominal composition, is a frequent feature; domains of regular intergrowth between n' = 6 and n = 7 have been observed leading to an n' = 6.5 complex member. The close relationships with the 2201 modulated superconducting phase is illustrated through the coexistence of the two structural types in the same crystal, without strong distortions of the framework. The absence of superconducting properties can be compared to the behavior of $Bi_{17}Sr_{16}Cu_7O_{49-x}$, and correlated with the absence of infinite $[CuO_2]_\infty$ layers. The investigation of the other members of the "collapsed" family and of the nonstoichiometric mechanisms setting up in these matrices can be very beneficial for the understanding of the parameters which govern the superconducting properties of the bismuth cuprates.

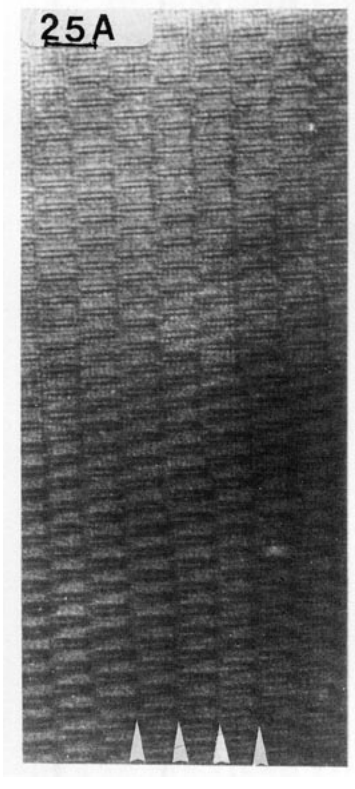

FIG. 14. [010] image: the variation of the n' members involve undulating boundaries (marked by white triangle).

References

1. C. MICHEL, M. HERVIEU, M. M. BOREL, A. GRANDIN, F. DESLANDES, J. PROVOST, AND B. RAVEAU, *Z. Phys. B* **68,** 421 (1987).
2. G. VAN TENDELOO, H. W. ZANDBERGEN, J. VAN LANDUYT, AND S. AMELINCKX, *Appl. Phys. A* **46,** 233 (1988).
3. E. KAKAYAMA, E. MUROMUCHI, Y. UCHIDA, A. ONO, F. IZUMI, AND M. ONODA, *Jpn. J. Appl. Phys.* **27,** L365 (1988).
4. P. L. GAI AND P. DAY, *Physica C* **152,** 335 (1988).
5. B. RAVEAU, C. MICHEL, M. HERVIEU, AND J. PROVOST, *Physica C* **153** (155), 3 (1988).
6. C. TORARDI, M. A. SUBRAMANIAN, J. C. CALABRESE, J. GOPALAKRISHNAN, E. M. MC CARRON, K. J. MORRISSEY, T. R. ASHEW, R. B. FLIPPEN, U. CHOWDRY, AND A. W. SLEIGHT, *Phys. Rev. B* **38,** 225 (1988).
7. H. VON SCHNERING, L. WALZ, M. SCHWARZ, W. BECKER, M. HARTWEG, T. POPP, B. HETTICH, P. MÜLLER, AND G. KÄMPF, *Angew. Chem. Int. Ed. Engl.* **27,** 574 (1988).
8. K. IMAI, I. NAKAI, T. KAWASHIMA, S. SUENO, AND A. ONO, *Jpn. J. Appl. Phys.* **27,** 1661 (1988).
9. H. LELIGNY, S. DURCOK, P. LABBE, M. LEDESERT, AND B. RAVEAU, *Acta Crystallogr.*, in press.
10. Z. HIROI, Y. IKEDA, M. TAKANO, AND Y. BANDO, *J. Mater. Res.* **6,** 435 (1991).
11. Y. MATSUI, S. TAKEKAWA, K. KISHIO, A. UMEZONO, S. NAKAMURA, C. TSURUTA, AND K. IBE, *Mater. Trans. JIM* **31,** 595 (1990).
12. A. FUERTES, C. MIRATVILLES, J. GONZALEZ CALBERT, M. VALLET REGI, AND J. RODRIGUEZ CARJAVAL, *Physica C* **157,** 529 (1989).

13. M. T. Caldes, J. M. Navarro, F. Perez, M. Carrera, J. Fonturba, M. Casan Pastor, C. Miratvilles, X. Obradors, J. Rodriguez Carjaval, J. M. Gonzalez-Calbert, M. Vallet Regi, A. Garan, and A. Fuertes, *Chem. Mater.* **3,** 844 (1991).

14. M. T. Caldes, M. Hervieu, A. Fuertes, and B. Raveau, *J. Solid State Chem.* **97,** 48 (1992).

15. M. T. Caldes, M. Hervieu, A. Fuertes, and B. Raveau, *J. Solid State Chem.* **98,** 301 (1992).

16. M. T. Caldes, M. Hervieu, A. Fuertes, and B. Raveau, *J. Solid State Chem.* **98,** 48 (1992).

17. A. Q. Pham, M. Hervieu, C. Michel, and B. Raveau, *J. Solid State Chem.* **98,** 426 (1992).

18. A. Q. Pham, C. Michel, M. Hervieu, A. Maignan, and B. Raveau, *J. Phys. Chem. Solids* **54,** 65 (1993).

19. H. W. Zandbergen, W. A. Groen, F. C. Mijlhoff, G. Van Tendeloo, and S. Amelinckx, *Physica C* **156,** 325 (1988).